Skeletal Radiology (2019) 48:57–74
https://doi.org/10.1007/s00256-018-3028-z

REVIEW ARTICLE

Sonographic evaluation of uncommonly assessed upper extremity peripheral nerves: anatomy, technique, and clinical syndromes

Jonathan M. Youngner[1] · Kulia Matsuo[1] · Tom Grant[1] · Ankur Garg[1] · Jonathan Samet[1,2] · Imran M. Omar[1]

Received: 10 January 2018 / Revised: 13 June 2018 / Accepted: 17 June 2018 / Published online: 23 July 2018

Abstract

Targeted ultrasound of the median, ulnar, and radial nerves is a well-established technique for suspected upper extremity peripheral neuropathy. However, sonographic imaging of the brachial plexus and smaller peripheral nerve branches is more technically difficult and the anatomy is less familiar to many radiologists. As imaging techniques improve, many clinicians refer patients for imaging of previously less-familiar structures. In addition, some patients may present with injuries that could involve local neurovascular structures. Finally, patients presenting with isolated peripheral neuropathies may be referred for perineural injections with local anesthetic for diagnostic purposes, or steroid for therapeutic reasons. This requires sonologists to have a firm understanding of the courses of these nerves and the surrounding anatomic landmarks that can be used to accurately identify and characterize them. We discuss clinical syndromes referable to specific peripheral nerve branches in the upper extremity, the relevant anatomy, and sonographic technique.

Keywords Ultrasound · Peripheral nerve · Perineural injection

Introduction

The major peripheral nerves of the upper extremity may be injured by tumor, penetrating trauma, iatrogenic causes, or in the setting of overuse syndromes. Ultrasound has the capability to identify subtle peripheral nerve abnormalities in the absence of electrodiagnostic findings, such as in clinically diagnosed carpal tunnel syndrome [1]. Nerve entrapment within fibro-osseous tunnels such as Guyon's canal and the cubital and carpal tunnels are well known entities to most radiologists who routinely perform musculoskeletal ultrasound [2]. Additionally, the relatively large caliber of these nerves makes them readily identifiable [3]. In contradistinction, the brachial plexus and upper extremity peripheral nerve branch anatomy is more complicated and less commonly encountered in daily clinical practice. Furthermore, the small caliber of peripheral nerve branches makes them more difficult to identify and differentiate from surrounding tissues.

Normal peripheral nerves may be readily identified by their characteristic echotexture, differentiating them from surrounding connective tissue, tendons, and vessels. High-frequency (12–18 MHz) linear transducers optimize spatial resolution when evaluating these superficial structures. Occasionally, the authors have found that the added spatial resolution of a higher frequency transducer, such as a 24-MHz transducer (Toshiba Aplio i800, Irvine, CA, USA) may provide additional information about the fascicular architecture of superficial peripheral nerves or their surrounding structures. Small footprint transducers such as a "hockey stick" transducer may be helpful when evaluating nerve branches in the hand or wrist where the surface anatomy complicates use of a standard linear transducer. Hypoechoic fascicles are surrounded by hyperechoic epineurium and perineurium. In short axis this results in a honeycombed, fasciculated appearance, which helps distinguish nerves from surrounding connective and soft tissue (Fig. 1a). Once a nerve is identified in short axis, it is best followed proximally or distally in short axis. A site of suspected pathology can then be further characterized by imaging the nerve in long axis [3]. In the long axis, normal nerves demonstrate a parallel arrangement of tubular hypoechoic fascicles with interspersed linear areas of

✉ Jonathan M. Youngner
jonathan.youngner@northwestern.edu

[1] Department of Radiology, Feinberg School of Medicine, Northwestern University, 676 N. St. Clair St. Ste 800, Chicago, IL 60616, USA

[2] Department of Radiology, Lurie Children's Hospital, Chicago, IL, USA

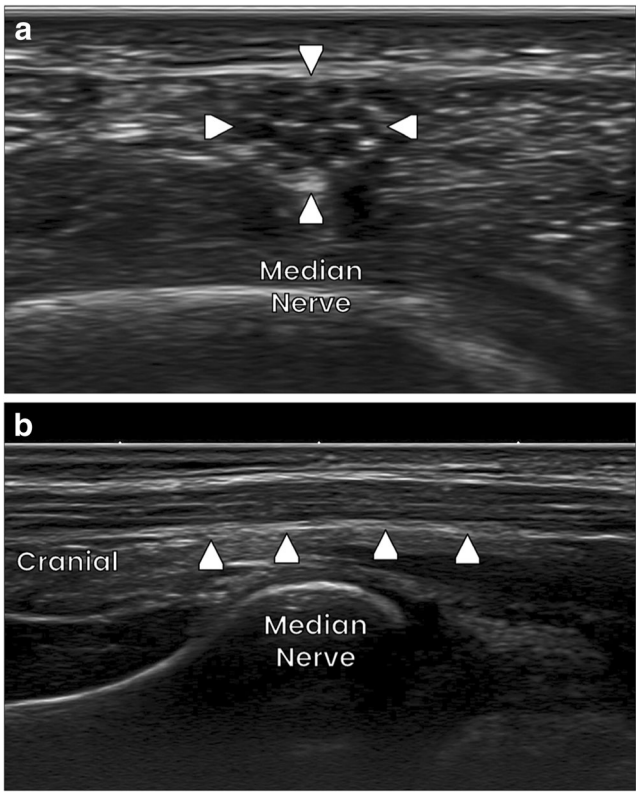

Fig. 1 Normal sonographic appearance of a nerve. Transverse (**a**) and longitudinal (**b**) sonographic images of the median nerve (*arrowheads*) obtained at the level of the wrist with a 24-MHz transducer demonstrate the normal honeycombed, fasciculated appearance typical of peripheral nerves

echogenic connective tissue (Fig. 1b). This distinct echotexture allows differentiation from tendons, that appear more fibrillated and hyperechoic. Peripheral nerve pathology may manifest as abnormal course or caliber, disrupted fascicular architecture or echogenicity, or frank discontinuity of a nerve [4]. It should be noted that anisotropy is a potential pitfall when imaging peripheral nerves. Proper sonographic technique requires a perpendicular angle of insonation with respect to the nerve. If the nerve is imaged even slightly off of the perpendicular, fewer sound waves are reflected back to the transducer resulting in a falsely hypoechoic appearance of the nerve [5]. Finally, comparison to the contralateral, asymptomatic upper extremity may enhance the sonologist's diagnostic confidence regarding a particular finding associated with the nerve of interest [6].

Peripheral nerve evaluation with ultrasound may be more limited when imaging deep structures, possibly necessitating a lower frequency probe. Furthermore, gas, bone, and surgical material may create artifact that obscures evaluation of the target nerve. Knowledge of sonographic landmarks, particularly osseous landmarks, can aid in identifying peripheral nerves and guiding procedures, such as image-guided peripheral nerve blocks. In cases of motor nerve pathology, the muscles supplied by a particular affected nerve may become atrophied and fatty infiltrated, which can be detected sonographically. Thus, the distribution of affected muscles can suggest a particular peripheral neuropathy even if the nerve of interest demonstrates a normal sonographic appearance. We describe the relevant anatomic landmarks that may be utilized to evaluate less commonly assessed upper extremity peripheral nerve branches and present cases of peripheral nerve pathology along with a discussion of their associated clinical syndromes.

Ultrasound-guided peripheral nerve perineural injections

Ultrasound-guided perineural injection of local anesthetic is a well-established technique amongst anesthesiologists to achieve regional anesthesia for upper extremity surgery [7]. Radiologists also often perform upper extremity peripheral nerve perineural injections for diagnostic purposes utilizing local anesthetic or for therapeutic purposes utilizing steroids. Standard sterile technique, including draping the ultrasound transducer with a sterile cover, is utilized for these injections. We typically utilize a 25-gauge needle for these injections, although a 22-gauge spinal needle may occasionally be used if a longer needle trajectory is necessary. The nerve in question may be identified utilizing the landmarks and techniques discussed in this review. Next, the needle trajectory should be determined with care to avoid vessels, tendons, and other vital structures that could be injured during needle insertion.

Two needle approaches commonly used are the "in-plane" and "out-of-plane" techniques. The "in-plane" technique involves positioning the ultrasound probe transversely with respect to the nerve so that a "short-axis" view of the nerve is obtained. The needle tip is then advanced in parallel to the probe's long axis (Fig. 2a). The "out-of-plane" approach involves advancing the needle perpendicular to the probe's long axis. The "in-plane" approach is preferred because the entire length of the needle is visualized during the injection (Fig. 2b). With the "out-of-plane" approach, only the needle tip is well visualized, appearing as an echogenic "dot", and the depth of the needle is more difficult to accurately assess [8]. Occasionally, a small anatomic window due to adjacent vascular structures or other regional anatomy precludes the longer needle trajectory required by the "in-plane" approach. In these cases, the "out-of-plane" approach is a valuable technique for proceduralists, for example when accessing the small joints of the hands (Fig. 2f). The authors routinely utilize color Doppler in order to distinguish small vessels from peripheral nerve branches.

Once the needle trajectory is determined, 1% lidocaine may be used to achieve cutaneous/subcutaneous anesthesia and the needle should be advanced to a perineural location with the needle bevel facing the nerve. We typically perform a

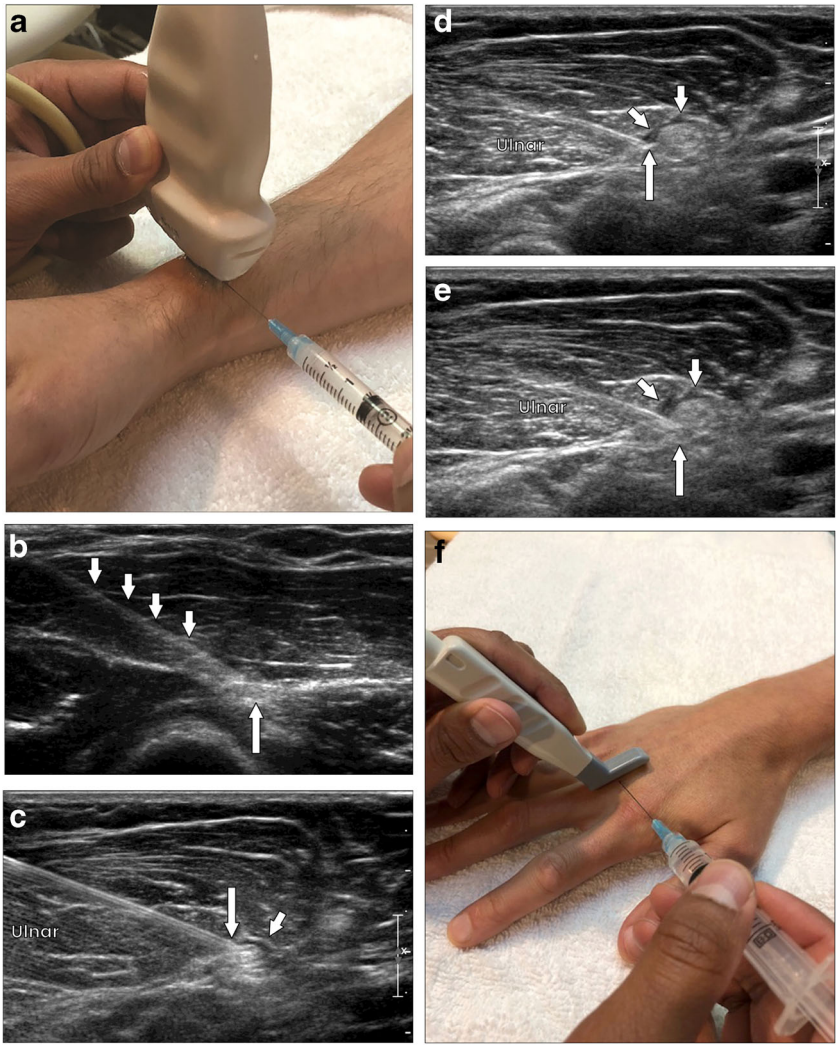

Fig. 2 Perineural injection in a 42-year-old male with Wartenberg's syndrome who was referred for perineural steroid injection. **a** Transducer and needle positioning for perineural injection of the superficial branch of the radial nerve utilizing the "in plane" approach. **b** "In plane" approach with a 22-gauge needle (*short arrows*) demonstrates perineural location of the needle in order to perform a test injection around the nerve (*long arrow*). **c** Test injection with 1% lidocaine demonstrates a small hypoechoic collection (*short arrow*) adjacent to the superficial branch of the radial nerve confirming the needle tip's perineural location (*long arrow*). **d**, **e** Injection of a mixture of 1% lidocaine and 40 mg triamcinolone results in a hypoechoic halo (*short arrows*) surrounding the nerve with the needle tip (*long arrow*) in a perineural location. **f** Transducer and needle positioning for "out of plane" approach to the metacarpophalangeal joint

perineural test injection with 1% lidocaine to confirm free epineural flow of injectate (Fig. 2c). The patient should not experience pain at any point during the procedure, which could indicate intraneural positioning of the needle. If this occurs, the needle tip should be adjusted in order to achieve epineural positioning before proceeding. Once epineural positioning of the needle tip is confirmed, the injection may be performed with longer acting local anesthetic and/or steroids [9]. Anesthesiologists typically inject a volume of 3–5 ml to achieve regional anesthesia [8]. Smaller volumes are typically required for diagnostic or therapeutic purposes. The desired result is a hypoechoic halo of injectate surrounding the nerve. Repositioning of the needle may be required to achieve circumferential perineural injection.

Corticosteroid selection may differ between institutions although triamcinolone and betamethasone are most commonly utilized. Although both preparations contain particulate steroids, betamethasone also comprises a soluble component. While this increased solubility may decrease potential cutaneous/subcutaneous side effects, it also decreases duration of activity in the soft tissues [10]. The authors prefer to include triamcinolone in our perineural injections due to its longer duration of activity in the perineural soft tissues. At our institution, we typically inject 1–2 ml of .75% bupivacaine for diagnostic purposes or a 2 ml mixture of .75% bupivacaine and 40 mg triamcinolone for therapeutic injections.

The patient may experience numbness and/or weakness in the expected nerve distribution, indicating a successful injection. The risk of direct nerve damage should be discussed with the patient; however, adhering to the technique and precautions we describe here mitigates this risk. Cosmetic considerations should also be discussed with the patient, particularly when performing perineural injections close to the skin surface. As the needle is withdrawn, leakage of steroid into the subcutaneous tissues could potentially result in atrophy of the subcutaneous fat or alterations in skin pigmentation [10]. Although rare, the authors mitigate this potential risk by flushing the needle with additional local anesthetic at the conclusion of the injection.

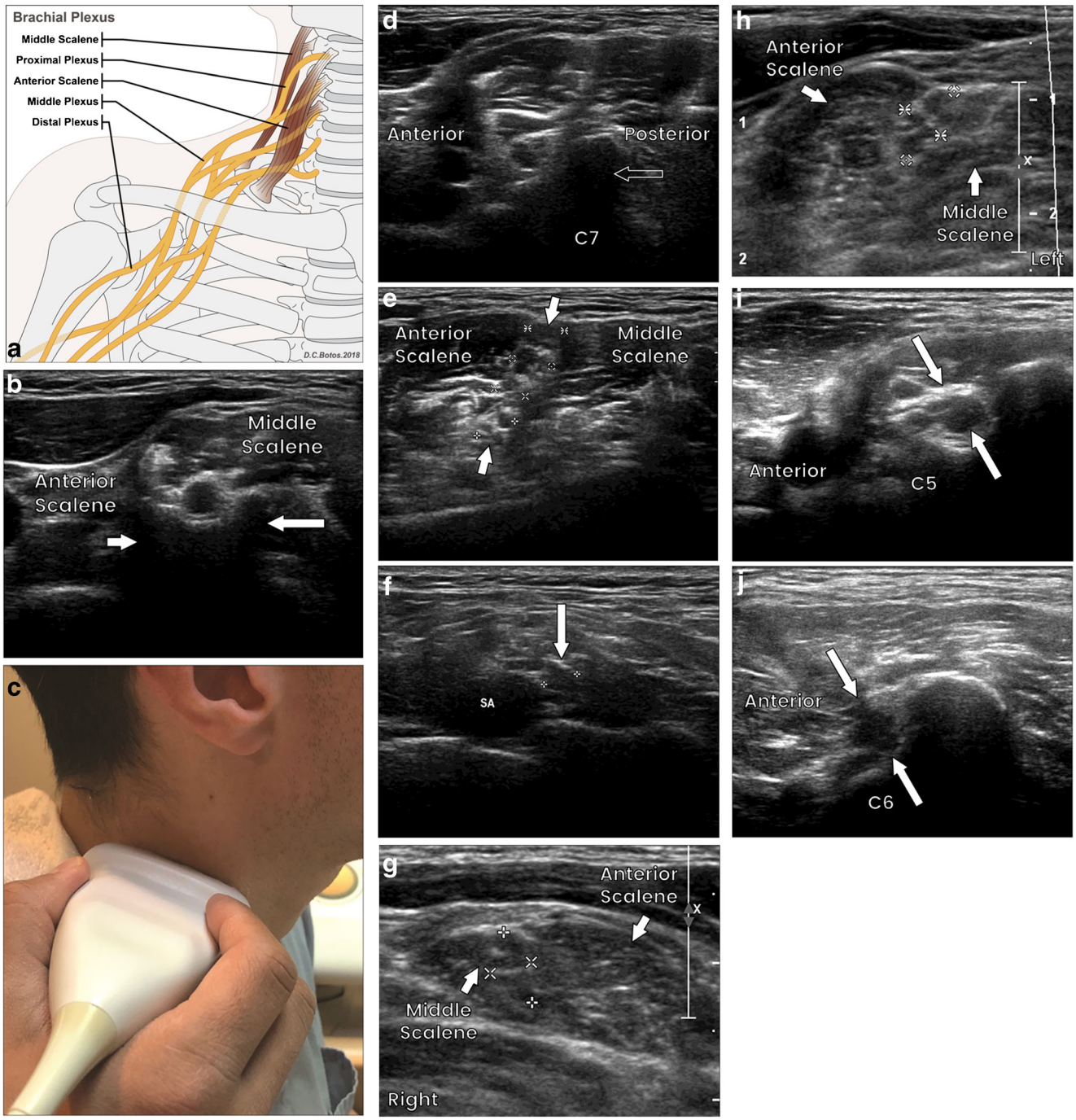

Fig. 3 Brachial Plexus. **a** Anatomy. **b** Transverse sonographic image of a normal brachial plexus demonstrates the relatively diminutive and symmetric anterior and posterior processes of the C6 vertebral body (*arrows*). **c** Transverse transducer positioning at the level of C7. **d** Corresponding sonographic image at the C7 level demonstrates the characteristic enlarged posterior process (*arrow*). **e** Transverse image of the brachial plexus (*arrows*) at the level of the interscalene groove. **f** Sonographic image at the periclavicular level demonstrates the subclavian artery (SA) with overlying "cap" of a normal brachial plexus (*arrow*). **g** A 35-year-old woman presented with left neck pain and swelling. Targeted ultrasound demonstrates asymmetric enlargement of the left brachial plexus fascicles (*arrow*) as they exit the interscalene groove. **h** Normal caliber right brachial plexus fascicles (*arrow*) as they exit the interscalene groove on the unaffected side in the same patient. **i** A 23-year-old man presented for evaluation after suspected posttraumatic plexopathy and suspected nerve root traction injury. Ultrasound demonstrates a thickened and hypoechoic left C5 nerve root (*arrows*). **j** Normal caliber C6 nerve root in the same patient (*arrows*)

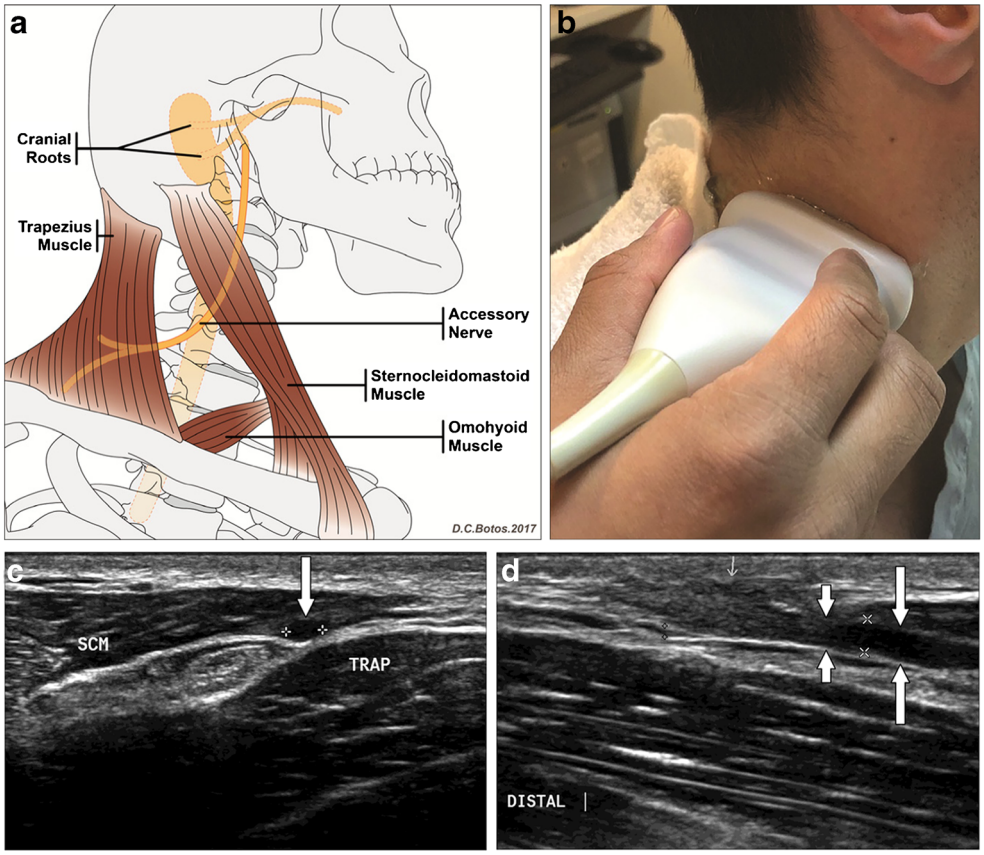

Fig. 4 Spinal accessory nerve **a** Anatomy. **b** Transducer positioned transversely with respect to the SAN. **c** Corresponding sonographic image demonstrates a normal SAN (*arrow*) traversing the posterior triangle of the neck between the sternocleidomastoid muscle (SCM) and trapezius muscle (TRAP). **d** 45-year-old male who suffered severe, but clinically incomplete left SAN injury during resection of a sebaceous cyst. Ultrasound of the left posterior triangle oriented in long axis with respect to the nerve demonstrates focal enlargement (*long arrows*) and suspected discontinuity (*short arrows*) of the SAN. Intraoperatively, the region of interest was characterized as a neuroma-in-continuity, electrical stimulation of the nerve demonstrated preserved nerve function, and neurolysis was performed

Specific nerves

Brachial plexus

The complex anatomy of the brachial plexus can be daunting for even the experienced sonographer. Standard brachial plexus anatomy comprises the ventral rami of the C5-T1 nerve roots, which then exit the cervical vertebral foramina and enter a groove between the anterior and middle scalene muscles. Peripherally they divide proximally into superior, middle, and inferior trunks (Fig. 3a). Nerve roots C5 and C6 contribute to the superior trunk, combining near the middle scalene muscle's medial border. The C7 root forms the middle trunk and roots C8 and T1 combine to form the inferior trunk. Each trunk divides into anterior and posterior divisions as they pass posterior to the mid clavicle, through the interscalene groove. The divisions combine to form lateral, posterior, and medial cords, which are named due to their relationship with respect to the axillary artery. The lateral cord comprises the anterior divisions of the superior and middle trunks; the posterior cord comprises the posterior divisions of all three trunks, and the medial cord comprises the anterior division of the inferior trunk. Finally, the terminal branches emerge from the cords. Specifically, the musculocutaneous nerve and lateral portion of the median nerve arise from the lateral cord, the radial and axillary nerves arise from the posterior cord, and the ulnar nerve and medial portion of the median nerve arise from the medial cord [11]. It should be noted that brachial plexus anatomy is highly variable, and may even vary from side to side in the same patient. A study of spontaneously aborted human fetuses demonstrated almost 54% variation from the standard brachial plexus anatomy with contributions from C4 and T2 accounting for the most common variants [12]. Other common variations include a C7 contribution to the musculocutaneous nerve, the musculocutaneous nerve contributing to the median nerve, or the long thoracic nerve piercing the middle scalene muscle [13].

Brachial plexopathy typically manifests with ipsilateral upper extremity pain, paresthesias, or weakness. The brachial plexus may be affected by a variety of underlying pathologies including inflammatory disorders such as idiopathic brachial neuritis (Parsonage–Turner syndrome), mass effect from metastatic disease or other tumors, intrinsic tumors of the brachial plexus such as nerve sheath tumors, radiation therapy, and trauma. Pain and motor weakness are the predominant clinical findings for many brachial plexopathies. Sensory symptoms may predominate in the setting of radiation-induced plexopathy and thoracic outlet syndrome [14].

Several key landmarks serve to simplify sonographic evaluation of the brachial plexus. The cervical spine transverse processes have anterior and posterior tubercles, between which the nerve roots pass as they exit the spinal canal. The

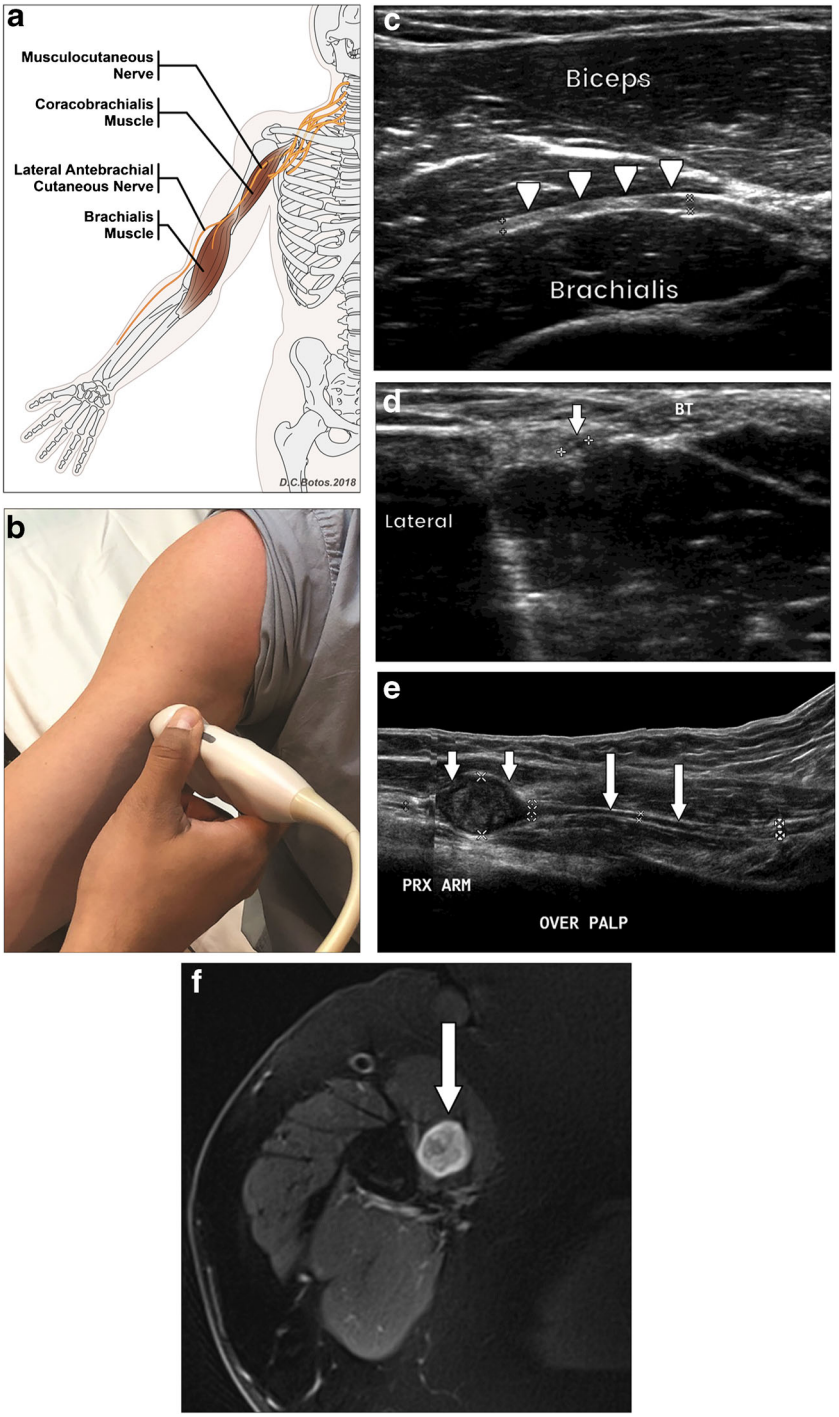

Fig. 5 Musculocutaneous Nerve **a** Anatomy **b** Transducer positioned transversely with respect to the musculocutaneous nerve in the upper arm. **c** Longitudinal sonographic image of the musculocutaneous nerve (*arrows*) in the mid upper arm coursing between the biceps and brachialis muscles. **d** Transverse sonographic image above the level of the elbow demonstrates a normal musculocutaneous nerve (*arrow*) lateral to the biceps tendon (BT). **e** A 43-year-old male presented with a palpable abnormality of the proximal upper arm. Longitudinal sonographic image over the palpable abnormality demonstrates an ovoid mass (*short arrows*) in continuity with the musculocutaneous nerve (*long arrows*). **f** Corresponding axial T2 fat-saturated MR image demonstrates the mass (*arrow*) located along the coracobrachialis muscle. The patient decided to be treated conservatively precluding a pathologic diagnosis, however the mass demonstrates a hyperintense rim and central hypointense signal consistent with a "target" sign typical of peripheral nerve sheath tumors. At a histologic level, the hyperintense rim is thought to comprise hypocellular Antoni type B cells while the central hypointense signal is a result of more cellular Antoni type A cells [19]

mid and lower cervical vertebrae typically demonstrate anterior and posterior processes that are similar in size (Fig. 3b). However, the C7 transverse process is recognizable since it has a larger posterior process and a diminutive anterior process (Fig. 3d). This morphology helps orient the sonographer to the appropriate cervical spine level when assessing brachial plexus pathology. More distally, the brachial plexus can be identified in the interscalene groove with the middle scalene muscle located posterior to the anterior scalene [15] (Fig. 3e). In the periclavicular region, the nerves of the brachial plexus form a "cap" over the artery, and can be found slightly cranial and posterior to the subclavian artery (Fig. 3f).

Spinal accessory nerve (SAN)

This motor nerve innervates the sternocleidomastoid (SCM) and trapezius muscles. Due to its superficial location, iatrogenic nerve injury may result from neck dissection. The nerve

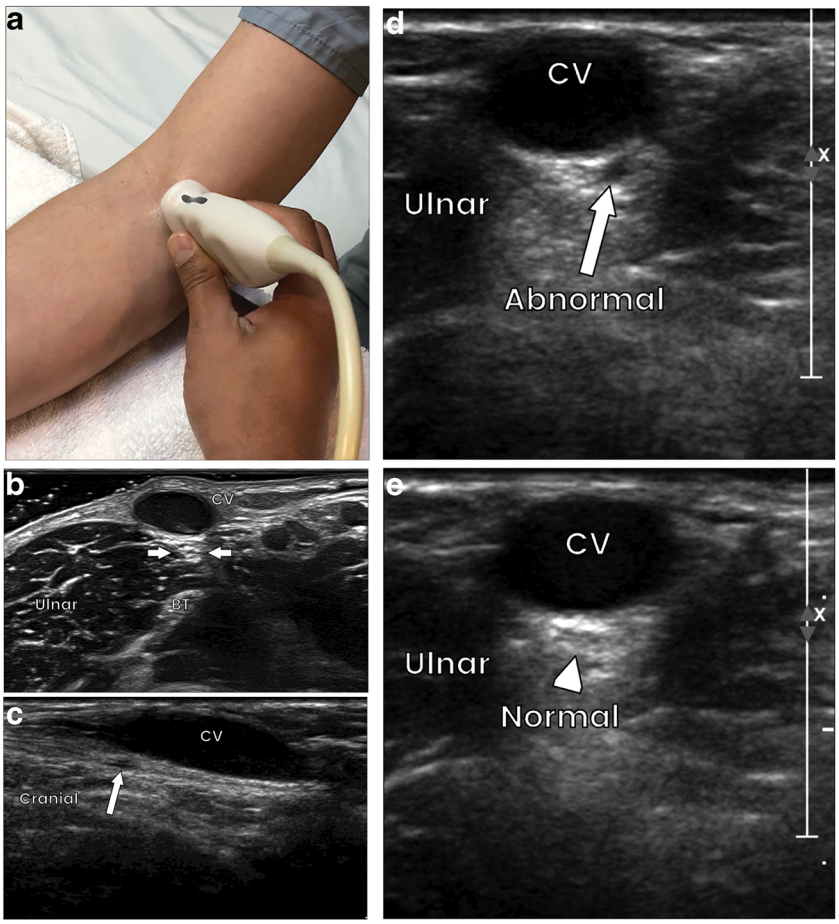

Fig. 6 LABN. **a** Transducer positioned transversely with respect to the nerve in the antecubital fossa. **b** Transverse sonographic image obtained with a 24-MHz transducer demonstrating a normal LABN (*arrow*) deep to the cephalic vein (CV) and superficial to the biceps tendon (BT). **c** Longitudinal sonographic image in a 38-year-old male who presented with suspected lateral antebrachial cutaneous nerve injury following venipuncture due to paresthesias in the expected nerve distribution. A normal appearing nerve is identified deep to the cephalic vein, however a focal hypoechoic segment (*arrow*) indicates the site of injury. **d** Transverse sonographic image in the same patient demonstrates the abnormal segment (*arrow*). The patient reported paresthesias with graded compression over this region, further supporting the clinical significance of this finding. **e** Comparison to the asymptomatic contralateral side in the same patient demonstrates a normal caliber nerve (*arrowhead*)

is intentionally resected during radical neck dissection, which can result in significant functional impairment [16]. Trapezius muscle atrophy may lead to shoulder girdle depression, scapular dyskinesis, and reduced active shoulder abduction. The SCM acts to elevate the rib cage during activities such as breathing. It also rotates the head to the contralateral side and flexes the head to the ipsilateral side. Dysfunction of this nerve can lead to an inability to rotate or flex the head to the side and difficulties in respiration [17]. SCM weakness is a sign of more superior SAN injury above the level of the posterior triangle. [18]. SAN sparing procedures such as modified radical and selective neck dissection aim to avoid these complications, although the nerve may be unintentionally injured during these surgeries as well. Direct blunt or penetrating trauma may also result in SAN impairment [16].

The SAN descends from the jugular foramen into the posterior triangle of the neck. This anatomic space is bounded superiorly by the confluence of the SCM and trapezius muscle, anteriorly by the SCM, posteriorly by the trapezius muscle, and inferiorly by the clavicle (Fig. 4a). Sonographically, the SAN can be found at the lateral posterior border of the SCM where it enters the posterior triangle and courses inferiorly between the SCM and the levator scapulae muscle. Distally, the SAN travels along the anterior border of the trapezius muscle in the lower third of the neck (Fig. 4c) [16].

Musculocutaneous nerve

The musculocutaneous nerve is one of the terminal branches of the lateral cord, generally receiving C5 and C6 nerve root fibers (Fig. 5a). It is a mixed sensory and motor nerve and provides motor innervation to the coracobrachialis, brachialis, and biceps brachii muscles before piercing the antebrachial fascia. After arising from the lateral cord, the nerve pierces the coracobrachialis muscle where it may be entrapped. It is susceptible to traction injuries, resulting in biceps brachii and brachialis muscle weakness and difficulties in elbow flexion [20]. More distally, it courses between the brachialis and biceps brachii muscles (Fig. 5c). On ultrasound, the nerve can be identified as it emerges between the brachialis and biceps brachii muscles and then courses lateral to the biceps brachii tendon above the level of the elbow (Fig. 5d). This nerve has a number of variations, such as receiving a contribution from the C7 nerve root as well as communicating with the median nerve. In a small number of patients the nerve may even be absent [21]. To perform a perineural injection the patient can be positioned with the arm abducted to 90 degrees and slightly

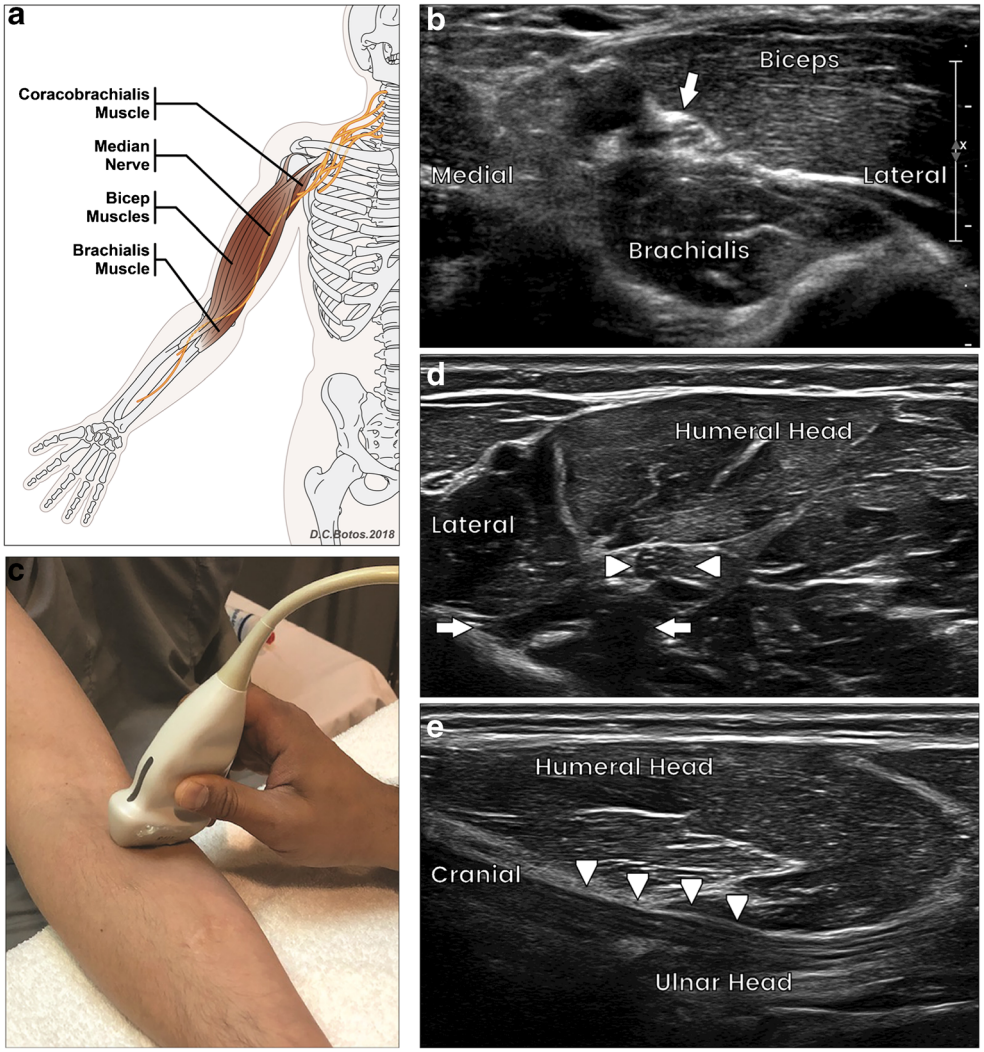

Fig. 7 Median Nerve **a** Anatomy **b** Transverse sonographic image just above the elbow demonstrates a normal median nerve (*arrow*) between the biceps and brachialis muscles. **c** Transducer positioned transversely with respect to the median nerve at the level of the elbow. **d** Corresponding transverse sonographic image obtained with a 24-MHz transducer at the level of the elbow demonstrates a normal median nerve (*arrowheads*) coursing between the humeral and ulnar (*short arrows*) heads of the pronator teres muscle. **e** Longitudinal sonographic image obtained with a 24-MHz transducer at the level of the elbow demonstrates a normal median nerve (*arrowheads*) coursing between the humeral and ulnar heads of the pronator teres muscle

externally rotated. The transducer is positioned along the short axis of the arm to give a cross-sectional image of the nerve. Once the nerve is identified the needle can be advanced using an anterior/cephalic in-plane approach through the biceps muscle to the margin of musculocutaneous nerve where the local anesthetic/steroid is injected.

Lateral antebrachial cutaneous nerve (LABN)

The musculocutaneous nerve gives rise to the LABN, which provides sensory innervation to the volar and radial aspects of the forearm (Fig. 5a). Injury to this nerve during venipuncture, distal humerus fracture, proximal radius fracture, and distal biceps tendon rupture or repair may result in pain or paresthesias along the lateral forearm. More proximal injury to the musculocutaneous nerve may result in mixed motor and sensory symptoms, with paresthesias along the distribution of the LABN. The LABN is identified by first placing the transducer transversely in the antecubital fossa and locating the biceps tendon. The nerve can be seen along the lateral superficial margin of the biceps tendon and deep to the cephalic vein in most cases [22] (Fig. 6b).

Pronator Teres syndrome

The median nerve is the other terminal branch of the lateral cord (Fig. 7a). It travels lateral to the brachial artery in the medial upper arm before entering the antecubital fossa deep to the bicipital aponeurosis. The nerve can be identified proximal to the elbow as it courses between the biceps brachii and brachialis muscles (Fig. 7b). The nerve then courses between the ulnar and humeral heads of the pronator teres muscle at the level of the elbow (Fig. 7d, e). Compression at this location may result in volar elbow or forearm paresthesias accompanied by pain. Similar symptoms in the hand may affect the 1st through 3rd digits and radial half of the 4th digit. Clinically, hand symptoms may be confused with carpal tunnel syndrome, however, Tinel's sign in the wrist may be absent in patients with pronator teres syndrome [23]. Focal manual compression over the pronator teres muscle may provoke

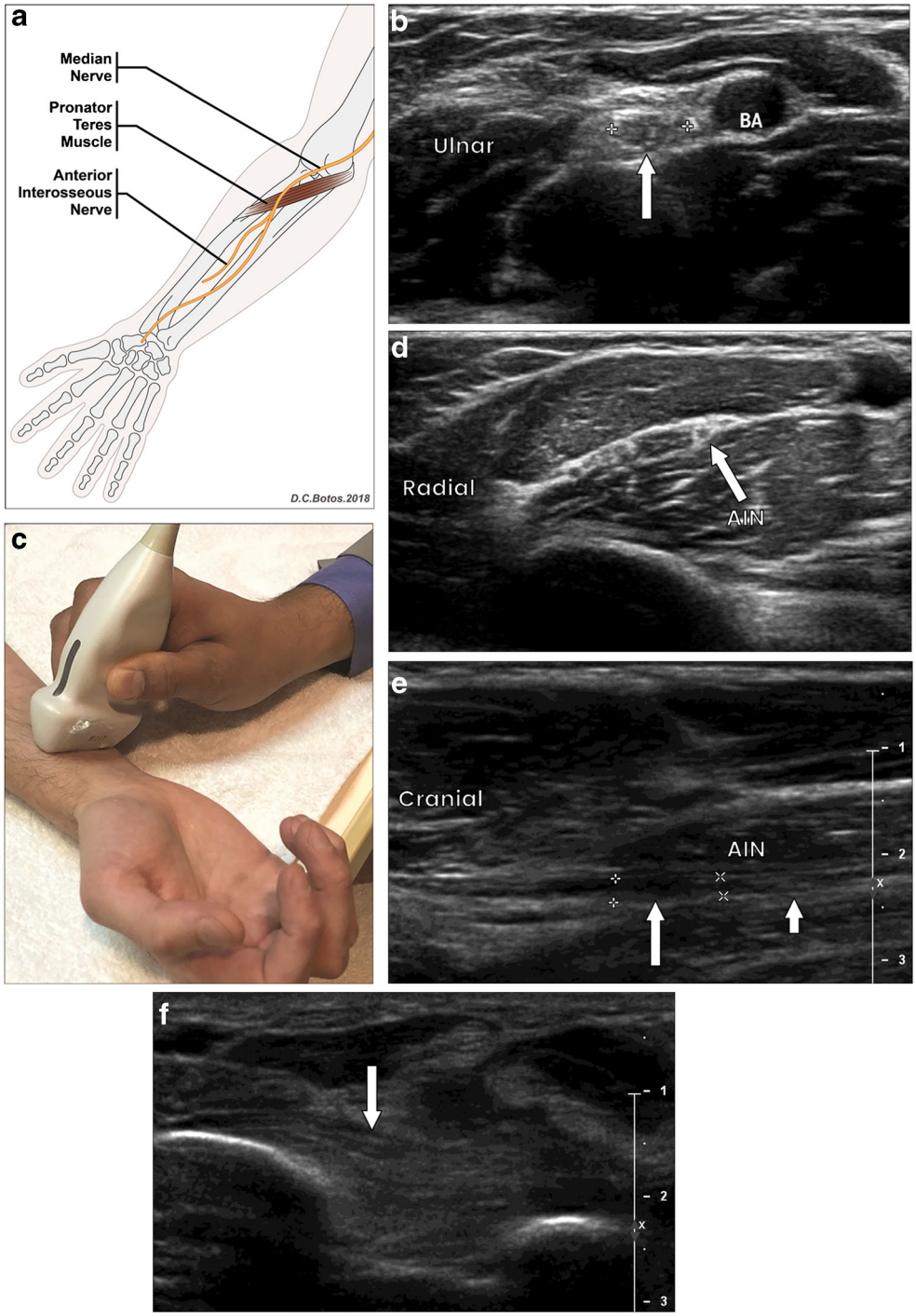

Fig. 8 Anterior interosseous nerve. **a** Anatomy. **b** Transverse sonographic image at the level of the antecubital fossa demonstrates a normal median nerve (*arrow*) ulnar to the brachial artery (BA). **c** Transducer positioned transversely with respect to the AIN in the distal forearm. **d** Transverse sonographic image more distally demonstrates a normal AIN (*arrow*). **e** Sonographic evaluation in a 50-year-old male who presented after a bicycle collision demonstrates a hypoechoic segment of the AIN (*long arrow*) with normalization distally (*short arrow*). **f** Transverse sonographic image in the same patient at the level of the distal forearm demonstrates increased echogenicity of the pronator quadratus (*arrow*) consistent with fatty infiltration secondary to denervation

symptoms in the affected arm and reproducible symptoms with resisted pronation of the forearm may provide further clinical evidence to support the pronator teres as the site of entrapment. Resisted elbow flexion with the elbow fully supinated can assess whether the lacertus fibrosis is the site of entrapment [24]. At the level of the elbow with the arm abducted and supinated, the median nerve can be located medial to the brachial artery. To perform a perineural injection the transducer can be positioned transverse to the long axis of the nerve in plane with the needle path. The needle can be advanced using an ulnar to radial approach to the surface of the nerve where the medications can be delivered [25]. Similarly, perineural injections of the median nerve can be performed more distally in the mid-forearm, distal to the anterior interosseous nerve and proximal to the palmar cutaneous branch of the median nerve. Perineural injections may be technically easier at this level than more proximal injections since the nerve does not generally closely travel with adjacent

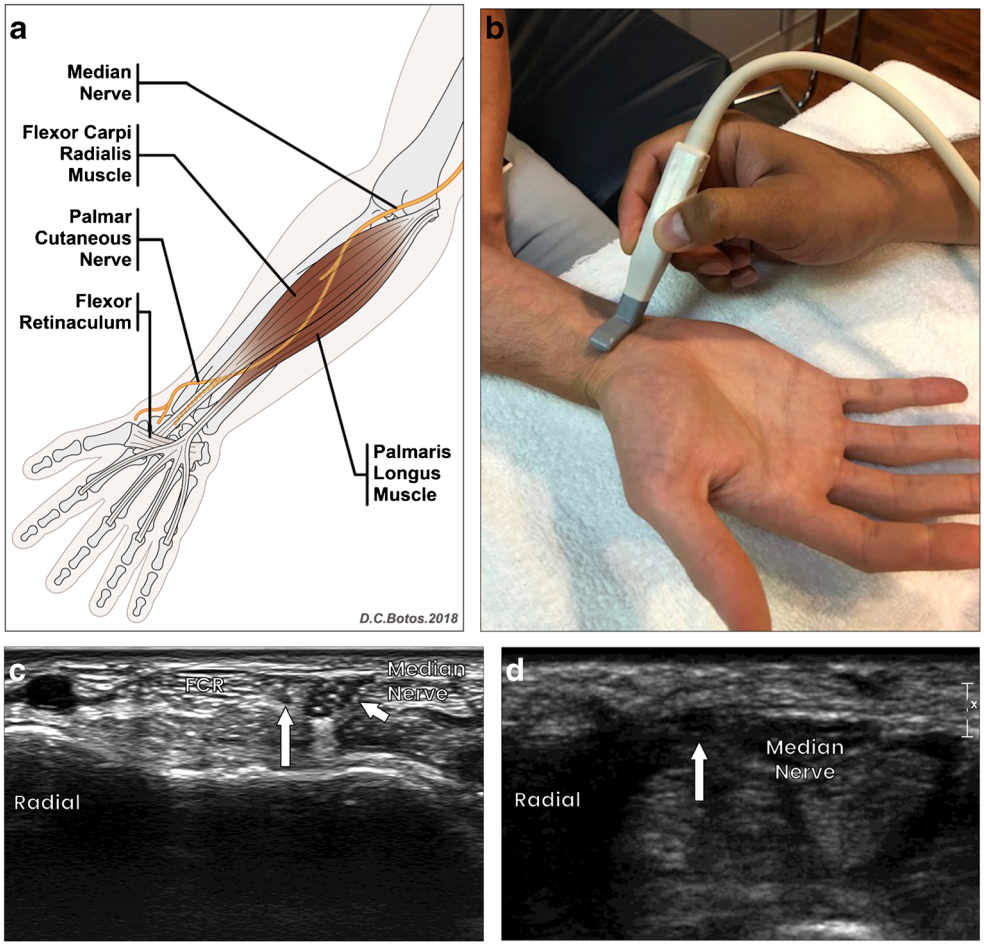

Fig. 9 Palmar cutaneous branch of median nerve **a** Anatomy **b** Transducer positioned transversely with respect the nerve proximal to the wrist. **c** Corresponding transverse sonographic image at the level of the distal forearm obtained with a 24-MHz transducer demonstrates a normal palmar cutaneous branch (*arrow*) along the radial aspect of the median nerve (MED NV) and adjacent to the flexor carpi radialis tendon (FCR). **d** Transverse sonographic image in a 35-year-old massage therapist who presented with thenar eminence pain, demonstrates an enlarged, hypoechoic palmar cutaneous branch (*arrow*), asymmetric when compared to the unaffected side (image not shown)

vessels. Using a transverse, in-plane approach the needle is advanced to the deeper margin of the nerve so that is directed away from any regional arteries. Once a portion of the injectate is administered the needle tip can be repositioned to the more superficial surface of the nerve to allow circumferential perineural injection [26].

Anterior interosseous nerve (AIN)

The median nerve gives rise to the AIN between the heads of the pronator teres muscle before it courses along the anterior interosseous membrane (Fig. 8a). The AIN is a motor nerve innervating the pronator quadratus, flexor pollicis longus, 2nd and 3rd flexor digitorum longus muscles. Enlargement of the bicipital bursa, repetitive elbow flexion, or compression between the pronator teres muscle heads may irritate this nerve leading to muscle weakness, denervation edema or atrophy, and inability to appose the 1st and 2nd digits [27]. Muscle weakness as opposed to paresthesias distinguishes this entity from pronator teres syndrome [24]. The transducer is placed transversely over the antecubital fossa to identify the median nerve, which is seen along the ulnar aspect of the brachial artery (Fig. 8b). Advancing the transducer distally enables visualization of the AIN as it arises at the level of the pronator teres muscle. Isolated atrophy and fatty infiltration of the pronator quadratus muscle may be seen in patients with AIN pathology (Fig. 8f).

Palmar cutaneous branch of the median nerve

This nerve branch arises in the distal forearm between the palmaris longus and flexor carpi radialis muscles before emerging from the flexor retinaculum (Fig. 9a). The palmar cutaneous branch most commonly arises 5 cm proximal to the wrist and courses ulnar to the flexor carpi radialis tendon between the flexor carpi radialis and palmaris longus tendons. The palmar cutaneous branch usually arises from the volar/radial surface of the median nerve. However, in a few people it may arise from the ulnar surface [28]. Rarely, it has been reported to cross the volar surface of the flexor carpi radialis tendon so that is courses radial to the tendon [29]. It is a sensory nerve innervating the mid proximal palm and thenar eminence. The nerve may be injured by direct trauma due to its superficial location and is also vulnerable to iatrogenic injury during carpal tunnel release, resection of volar ganglia,

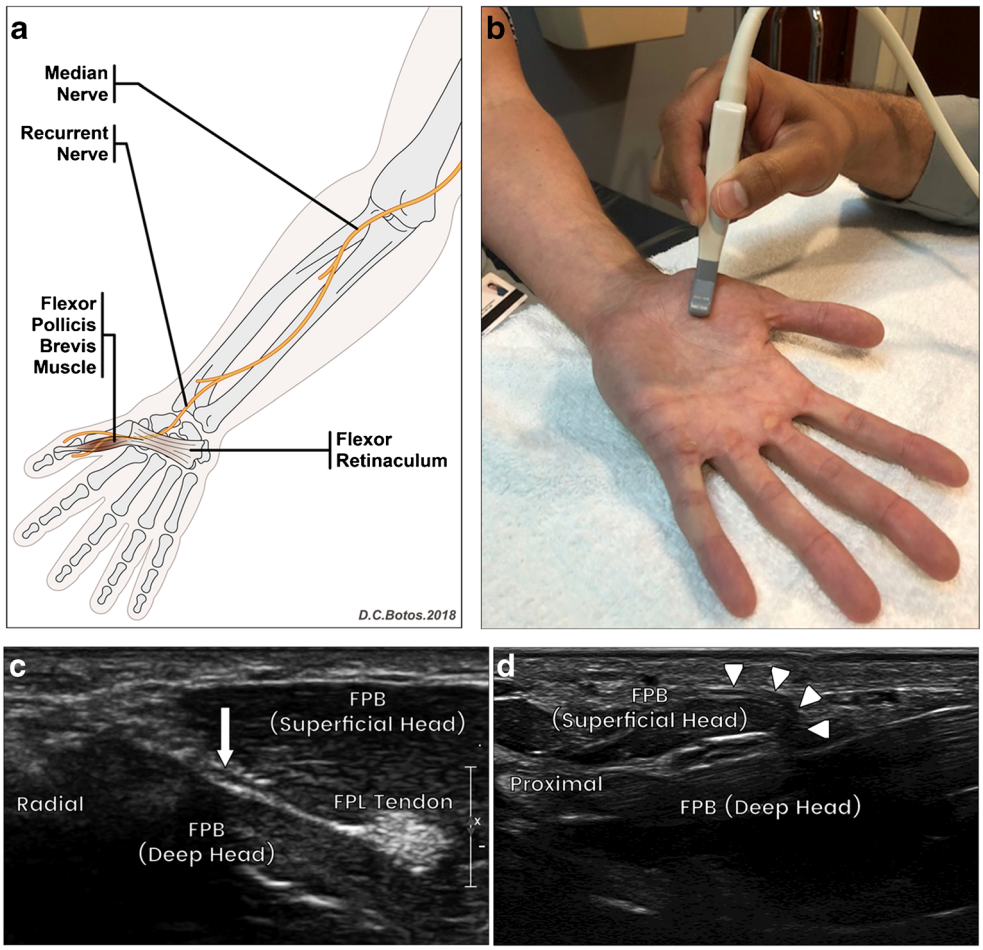

Fig. 10 Recurrent branch of median nerve **a** Anatomy **b** Transducer positioned transversely with respect to the recurrent branch. **c** Corresponding 24-MHz transverse sonographic image of a normal recurrent branch (*arrow*) after entering the thenar musculature deep to the superficial head of the flexor pollicis brevis muscle (FBP). **d** 24-MHz longitudinal sonographic image of a normal recurrent branch (*arrows*) as it dives into the thenar musculature

and tendon transfer. Hyperesthesias or sensory loss over the thenar eminence may indicate injury to this nerve [30]. Due to the fact that median nerve and palmar cutaneous branch pathology may result in a similar distribution of sensory impairment, ultrasound may help distinguish between these two entities in order to better target therapeutic management. To identify this branch, first identify the median nerve in the forearm as it passes between the flexor digitorum superficialis and flexor carpi radialis tendons (Fig. 9b). The palmar cutaneous branch arises from the radial aspect of the median nerve. As with other peripheral nerve perineural injections, the transducer is positioned along the short axis of the nerve and the needle is advanced to the margin of the nerve using an in-plane technique. Either a radial or ulnar needle approach may be selected.

Recurrent (thenar) branch of median nerve

This branch typically arises distal to the flexor retinaculum and provides motor innervation to the superficial head of the flexor pollicis brevis, abductor pollicis brevis, opponens pollicis, and occasionally the 1st dorsal interosseous muscle (Fig. 10a). A variant origin of the nerve within the carpal tunnel and trans-retinacular course of the nerve have been described [31]. Carpal tunnel release and compression by ganglia may injure this nerve resulting in isolated wasting of the thenar eminence [32]. Injury of this nerve can significantly impact the thenar musculature and decrease opposition of the thumb. The nerve is often referred to as the "million dollar nerve" since iatrogenic injuries have led to large monetary compensations following litigation. To identify this nerve, the median nerve should be identified in the carpal tunnel. The recurrent branch is usually found arising distal to the flexor retinaculum and typically from the volar or radial aspects of the median nerve. Occasionally, it may originate from the ulnar margin of the median nerve before entering the thenar musculature [31].

Palmar branch of the ulnar nerve

This branch nerve arises from the ulnar nerve in the distal forearm, approximately 5 cm proximal to the wrist (Fig. 11a). It can be identified within Guyon's canal, between the pisiform medially and the ulnar artery laterally (Fig. 11c). It then splits into deep motor and superficial sensory nerves within Guyon's canal [23]. Most commonly, this nerve may be

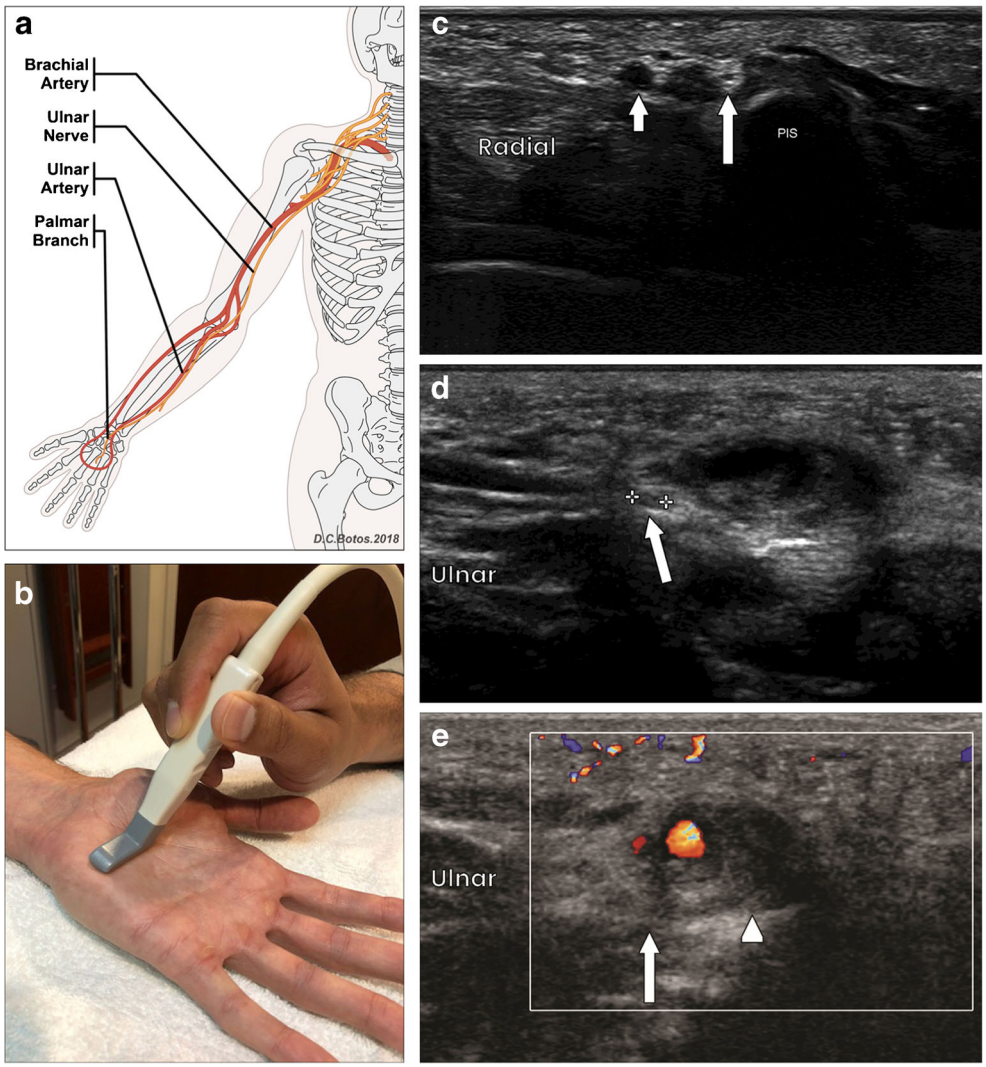

Fig. 11 Palmar branch of ulnar nerve **a** Anatomy **b** Transducer positioned transversely with respect to the palmar branch. **c** 24-MHz transverse sonographic image at the level of Guyon's canal demonstrates a normal palmar branch (*long arrow*) radial to the pisiform (PIS) and ulnar to the radial artery (*short arrow*). **d** Transverse sonographic image in a 30-year-old male hockey player who presented with pain and numbness after direct trauma with a hockey stick. The palmar branch (*arrow*) is identified adjacent to a partially hypoechoic mass. **e** Color Doppler interrogation demonstrates some residual flow within a partially thrombosed ulnar artery pseudoaneurysm (*arrowhead*) with mass effect on the palmar branch (*arrow*)

compressed by volar wrist ganglia. Usually these arise from the pisotriquetral joint or less commonly from the intercarpal joints [33]. Vascular lesions may also compress the nerve. Injury to this nerve variably results in motor, sensory or mixed symptoms depending on the level of injury [34].

Dorsal branch of the ulnar nerve

This branch arises in the distal forearm providing sensory innervation to the dorsal 5th digit as well as the dorsal and ulnar aspects of the 4th digit (Fig. 12a). Pain and paresthesias may result from trauma, ulnar osteotomy, or open reduction/internal fixation of ulnar fractures [35]. To identify this nerve, the ulnar nerve must be identified first in the mid ulna, deep to the flexor carpi ulnaris muscle (Fig. 12b). The nerve can then be followed distally to identify the dorsal branch that arises medially and courses along the medial aspect of the ulna (Fig. 12d).

Ulnar digital nerve of the thumb (bowler's thumb)

This sensory ulnar nerve branch innervates the ulnar aspect of the thumb (Fig. 13a). Repetitive compression of the nerve may result in development of perineural fibrosis that can lead to pain and paresthesias [36]. Bowlers are susceptible to this syndrome due to repetitive thumb abduction or compression stress on the thumb during release of the bowling ball. This

Fig. 12 Dorsal branch of ulnar nerve **a** Anatomy **b** Transverse sonographic image at the level of the mid ulna demonstrates a normal ulnar nerve (*arrow*) deep to the flexor carpi ulnaris muscle (FCU). **c** Transducer positioned transversely with respect to the dorsal branch in the distal forearm. **d** Corresponding transverse sonographic image demonstrates a normal dorsal branch (DORS BR) arising from the ulnar aspect of the ulnar nerve (UN). **e**, **f** A 40-year-old woman presented for ultrasound evaluation after distal forearm fracture. Longitudinal and transverse sonographic images of the dorsal branch demonstrate hypoechoic, fusiform thickening consistent with a post-traumatic neuroma (*arrows*). The distal nerve was poorly visualized and likely transected. Proximally, the ulnar nerve demonstrated normal caliber and echotexture (image not shown)

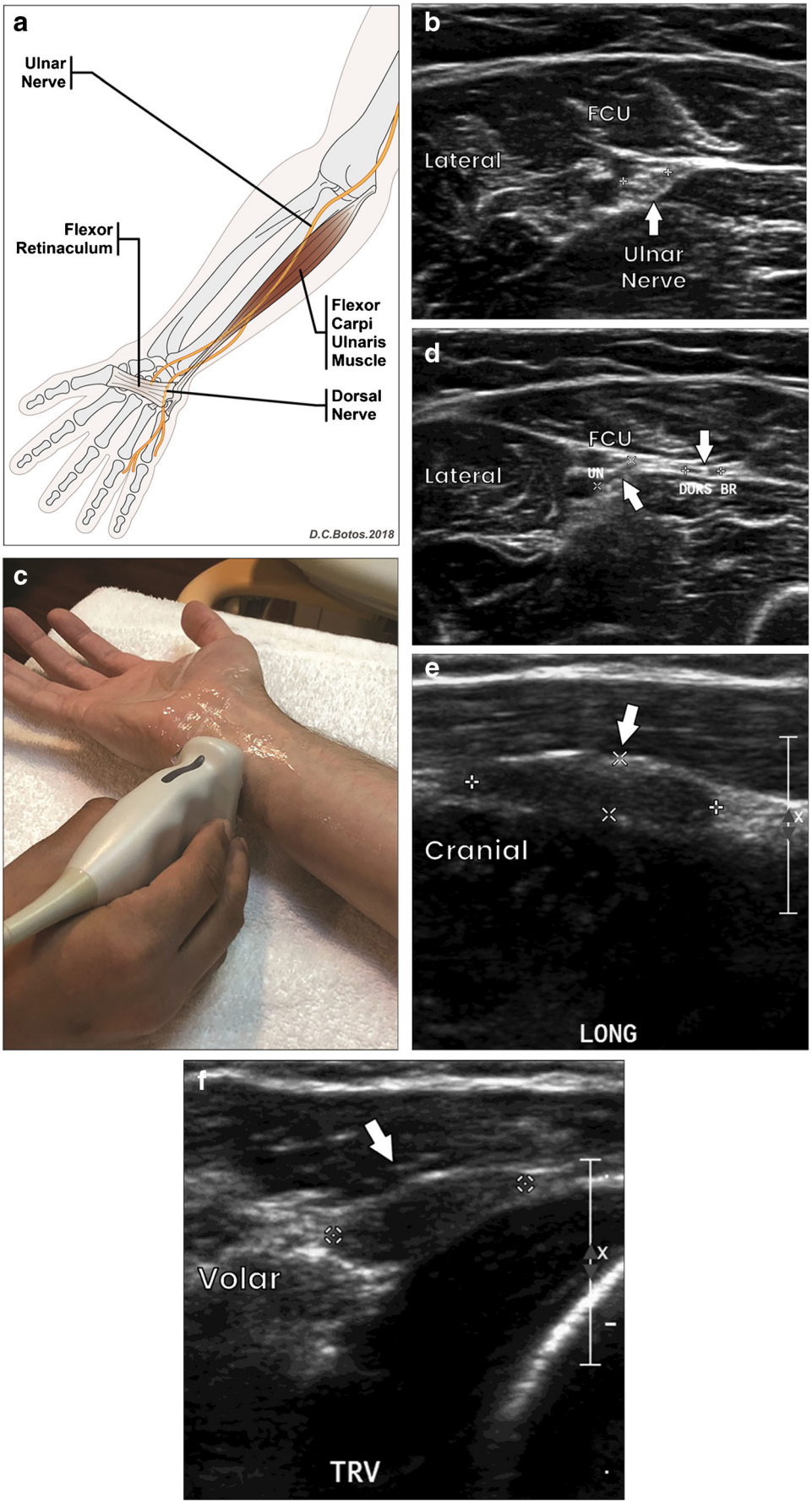
a
Ulnar Nerve
Flexor Retinaculum
Flexor Carpi Ulnaris Muscle
Dorsal Nerve
D.C.Botos.2018
b
FCU
Lateral
Ulnar Nerve
c
d
FCU
Lateral
UN
DORS BR
e
Cranial
LONG
f
Volar
TRV

may in turn lead to difficulties with hand grip, especially during pinching movements involving the thumb. To see this nerve one should identify the flexor pollicis longus tendon at the 1st MCP joint and move the transducer slightly ulnar to the tendon (Fig. 13c).

Superficial branch of the radial nerve (Wartenberg's syndrome or cheiralgia paresthetica)

This radial nerve branch arises at the elbow, courses deep to the brachioradialis muscle, and takes a superficial course in the distal forearm (Fig. 14a). Near its branch point the nerve is subfascial; however, it becomes more superficial by piercing the superficial fascia to become subcutaneous. The point of fascial penetration is about 8 cm proximal to the tip of the distal radial styloid process although this varies between 5 and 12 cm [37]. It is a sensory nerve innervating the 1st-3rd digits and radial aspect of the 4th digit. Radial fractures, fracture reduction, or compression of the wrist by handcuffs or a wristwatch may result in pain or paresthesias along the radial aspect of the wrist and thumb. This can be caused by a pincer effect between the brachioradialis and extensor carpi radialis longus tendons with forearm pronation or by fascial bands compressing the nerve. Intersection syndrome and De Quervain's tenosynovitis may present in a similar fashion, and therefore sonography may be indicated to distinguish between these entities [38]. In order to identify this nerve, one should first locate the radial nerve above the elbow between the brachialis muscle medially and the brachioradialis laterally. Then, the nerve should be followed distally to its bifurcation. The superficial branch courses deep to the brachioradialis muscle [39] (Fig. 14b).

Prior to a perineural injection it should be determined whether a subcutaneous or subfascial segment of the nerve is involved. Additionally, the site at which the nerve pierces the superficial fascia should be determined because the fascia may block the free passage of injectate along the nerve. If the precise site of neuropathy cannot be localized, some patients may benefit from injecting both subfascial and subcutaneous segments of the nerve [37].

Posterior interosseous nerve (PIN) syndrome

The deep motor branch of the radial nerve arises at the elbow adjacent to the lateral epicondyle. It pierces the supinator muscle and is referred to as the PIN after exiting the deep head of

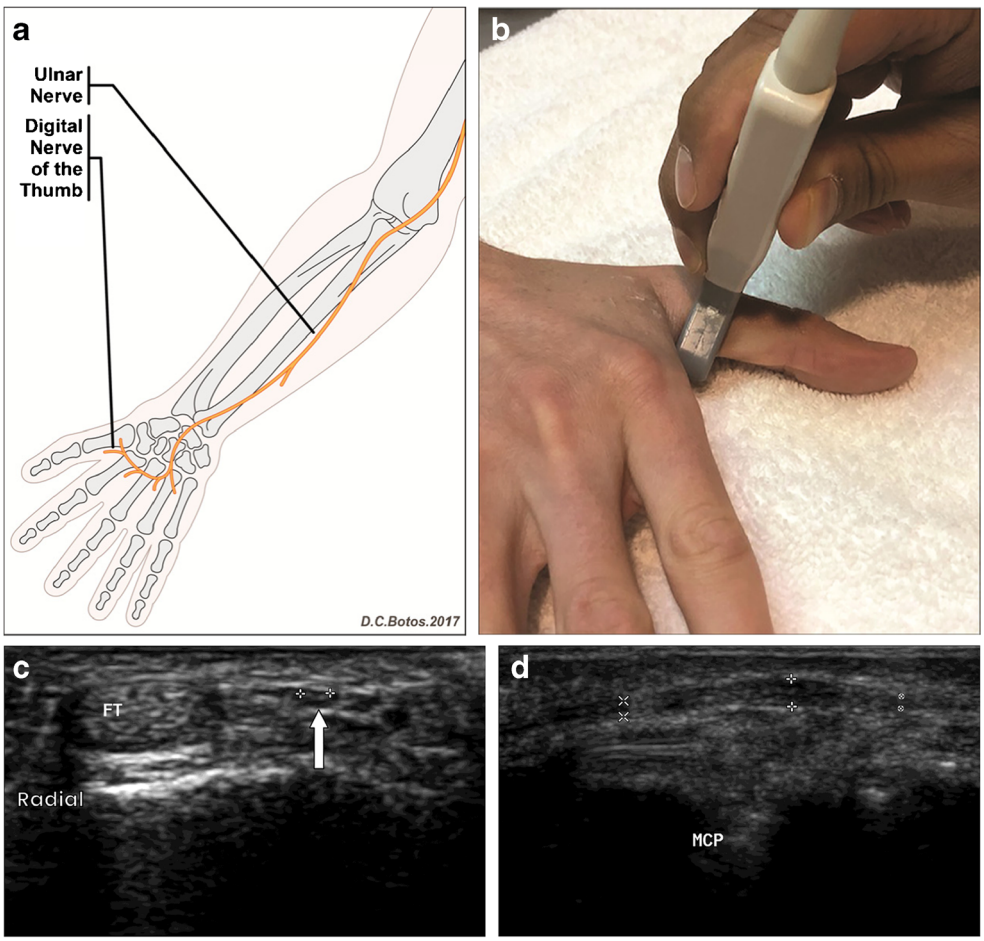

Fig. 13 Ulnar digital nerve of the thumb **a** Anatomy **b** Transducer positioned transversely with respect to the ulnar digital nerve. **c** Transverse sonographic image demonstrates a normal ulnar digital nerve (*arrow*) along the ulnar aspect of the flexor pollicis longus tendon (FT). **d** Longitudinal sonographic image in a 70-year-old male skier and tennis player with ulnar-sided paresthesias over the thumb demonstrates abnormal thickening of the ulnar digital nerve

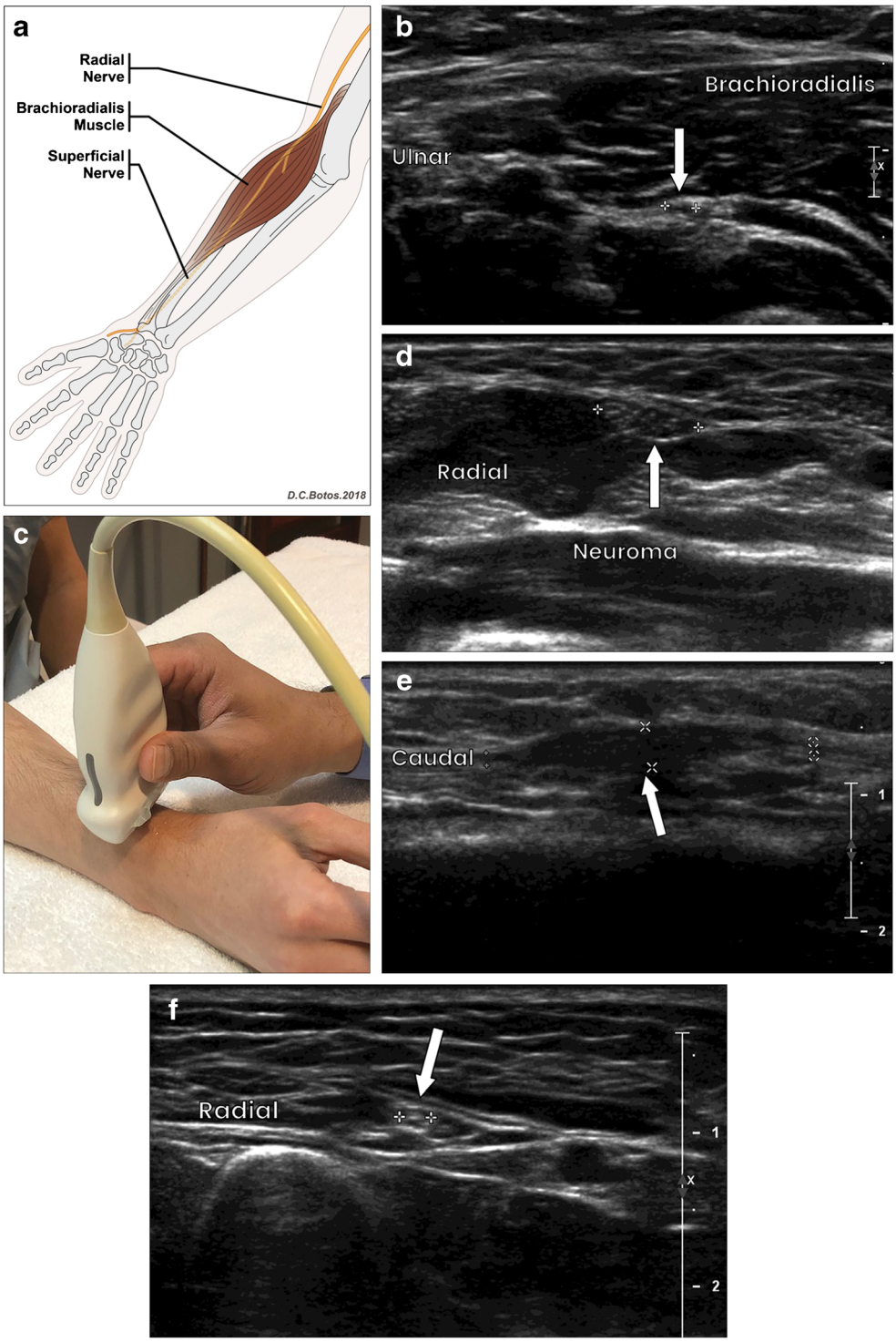

Fig. 14 Superficial branch of radial nerve **a** Anatomy **b** Sonographic image distal to the radial nerve bifurcation demonstrates a normal superficial branch (*arrow*) deep to the brachioradialis muscle. **c** Transducer positioned transversely with respect to the superficial branch in the distal forearm. **d**, **e** Transverse and longitudinal sonographic images in a 58-year-old man who presented with pain and paresthesias after remote injury demonstrates focal enlargement of the superficial branch (*arrows*) consistent with a post-traumatic neuroma-in-continuity. **f** More proximal transverse sonographic image in the same patient demonstrates normal caliber of the superficial branch (*arrow*)

the muscle after which it courses distally along the interosseous membrane to innervate the extensor muscles of the forearm. Compression of the nerve typically occurs at a tendinous thickening of the supinator muscle superficial head, referred to as the arcade of Frohse. Space occupying lesions such as ganglia and the leash of Henry, an arcade of recurrent radial artery branches that is slightly distal to the arcade of Frohse, may also result in PIN syndrome (Fig. 15a). The syndrome primarily consists of extensor muscle weakness in the forearm. Affected patients may have difficulty maintaining finger extension and radial deviation of the wrist may occur during wrist extension due to extensor carpi ulnaris

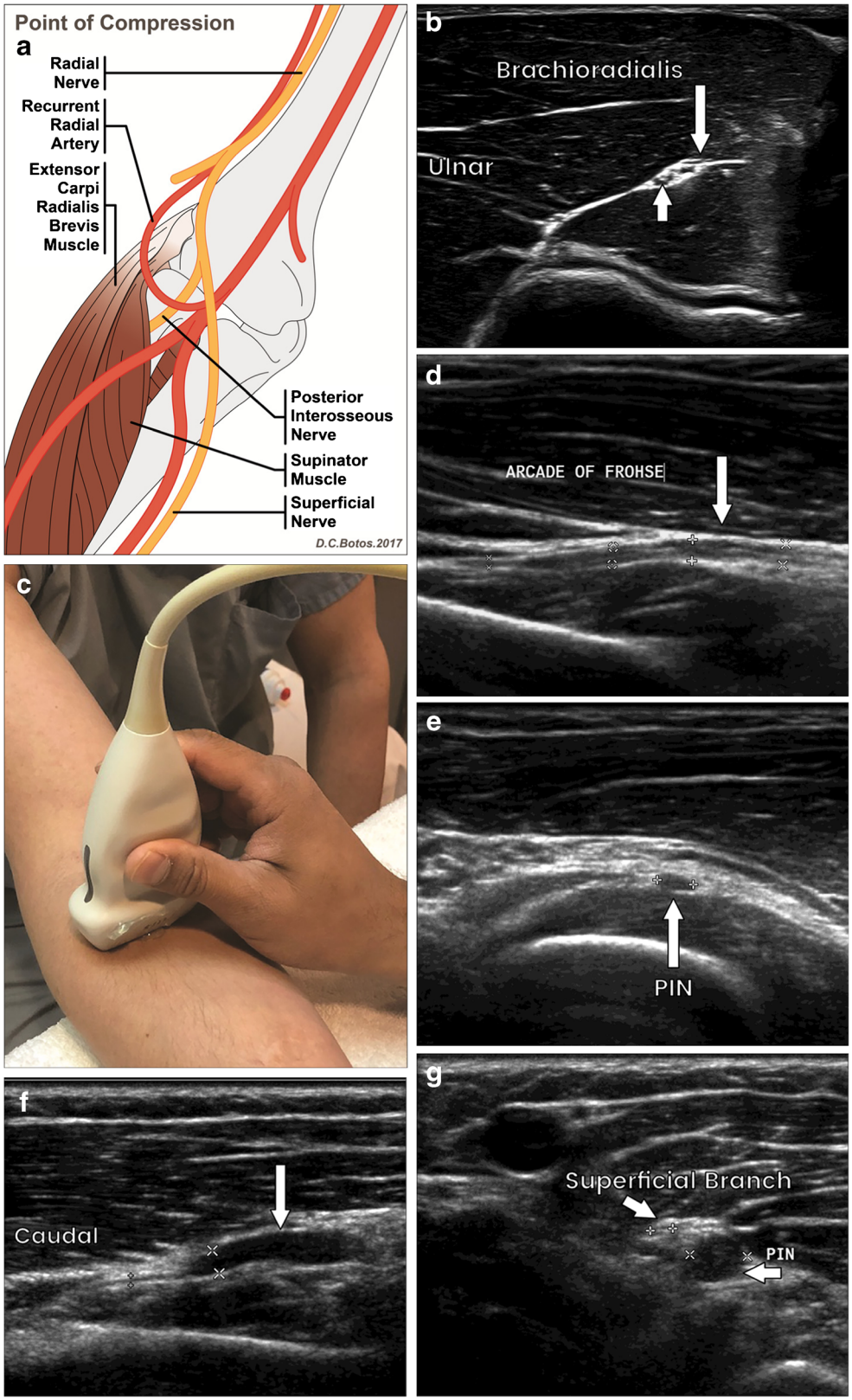

denervation. Pain may or may not accompany the motor symptoms. When a patient experiences pain it often occurs laterally and can mimic lateral epicondylitis that is recalcitrant to usual treatments for lateral epicondylitis. This entity has been referred to as "radial tunnel syndrome" [39]. In order to find the PIN, first identify the radial nerve above the elbow

◀ **Fig. 15** Posterior interosseous nerve. **a** Anatomy with points of potential compression. **b** 24-MHz transverse sonographic image at the level of the radial nerve bifurcation demonstrates a normal PIN (*long arrow*) and normal superficial branch (*short arrow*). **c** Transducer positioned transversely with respect to the PIN just distal to the elbow. **d** Longitudinal and **e** transverse sonographic images of a normal PIN (*arrow*) at the level of the arcade of Frohse. **f** Longitudinal sonographic image of the PIN in a 43-year-old man who presented with reduced grip strength and inability to extend the wrist demonstrates diffuse enlargement of the nerve from its origin to the arcade of Frohse (*arrow*). The nerve normalizes distally. **g** Transverse sonographic image in the same patient demonstrates the thickened PIN and adjacent normal caliber superficial branch

and follow it distally to its bifurcation into superficial and deep branches (Fig. 15b). The deep branch is the posterior interosseous nerve and can be seen piercing the arcade of Frohse (Figs 15d, e) [40]. It is important to follow the nerve distal to the supinator muscle to detect the second most common site of impingement at the leash of Henry.

In order to perform a perineural injection, the patient should be either supine or seated with the elbow slightly flexed and the thumb directed upward. The nerve should be localized in short axis between the heads of the supinator muscle and a medial to lateral, in-plane approach can be used at the site of flattening.

Conclusions

Sonographic evaluation of upper extremity peripheral nerve branches presents a challenge to radiologists. The relevant anatomy is complex and targeted evaluation of these small nerve branches is not routinely requested by referring physicians. Furthermore, the clinical syndromes associated with upper extremity peripheral nerve branch pathology are uncommonly encountered in daily practice and may be unfamiliar to many radiologists. A landmark-based anatomic approach enables relatively expedient sonographic identification of these nerve branches. Knowledge of these specific clinical syndromes enables the sonographer to customize the exam and increases the possibility of identifying clinically relevant nerve pathology. In this manner, a targeted evaluation may be tailored for each individual patient, thus increasing the efficacy and relevance of the diagnostic ultrasound examination. Furthermore, these landmarks may be utilized when performing ultrasound-guided perineural steroid or local anesthetic injections. It should be noted that variant nerve anatomy is relatively common. The landmark-based approach discussed in this review refers to standard anatomy and a tailored sonographic assessment in any individual patient may differ from the guidelines presented in this review.

References

1. Klauser AS, Halpern EJ, De Zordo T, Feuchtner GM, Arora R, Gruber J, et al. Carpal tunnel syndrome assessment with US: value of additional cross-sectional area measurements of the median nerve in patients versus healthy volunteers. Radiology. 2009;250(1):171–7.
2. Martinoli C, Bianchi S, Gandolfo N, Valle M, Simonetti S, Derchi LE. US of nerve entrapments in osteofibrous tunnels of the upper and lower limbs. Radiographics. 2000;20:S199–213.
3. Brown JM, Yablon CM, Morag Y, Brandon CJ, Jacobson JA. US of the peripheral nerves of the upper extremity: a landmark approach. Radiographics. 2016;36(2):452–63.
4. Yablon CM, Hammer MR, Morag Y, Brandon CJ, Fessell DP, Jacobson JA. US of the peripheral nerves of the lower extremity: a landmark approach. Radiographics. 2016;36(2):464–78.
5. Tagliafico A, Martinoli C. Reliability of side-to-side sonographic cross-sectional area measurements of upper extremity nerves in healthy volunteers. J Ultrasound Med. 2013;32:457–62.
6. Neal JM, Gerancher JC, Hebl JR, Ilfeld BM, McCartney CJ, Franco CD. Upper extremity regional anesthesia. Reg Anesth Pain Med. 2009;34(2):134–70.
7. Sehmbi H, Madjdpour C, Shah UJ, Chin KJ. Ultrasound-guided distal peripheral nerve block of the upper limb: a technical review. J Anasethesiol Clin Pharmacol. 2015;31(3):296–307.
8. Capek A, Dolan J. Ultrasound-guided peripheral nerve blocks of the upper limb. Continuing education in anaesthesia. Critical care & Pain. 2015;15:160–5.
9. Nwawka OK, Miller TT. Ultrasound-guided peripheral nerve injection techniques. AJR Am J Roentgenol. 2016;207(3):507–16.
10. Walter RW, Burke CJ, Adler RS. Ultrasound-guided therapeutic injections for neural pathology about the foot and ankle: a 4 year retrospective review. Skelet Radiol. 2017;46(6):795–803.
11. Orebaugh SL, Williams BA. Brachial plexus anatomy: normal and variant. Sci World J. 2009;9:300–12.
12. Uysal II, Seker M, Karabulut AK, Buyukmumcu M, Ziylan T. Brachial plexus variations in human fetuses. Neurosurg. 2003;53(3):676–84.
13. Emamhadi M, Chabok SY, Samini F, Alijani B, Behzadnia H, et al. Anatomical variations of brachial plexus in adult cadavers; a descriptive study. Arch Bone Jt Surg. 2016;4(3):253–8.
14. Khadilkar SV, Khade SS. Brachial plexopathy. Ann Indian Acad Neurol. 2013;16:12–8.
15. Lapegue F, Faruch-Bilfeld M, Demondion X, Apredoaei C, Bayol MA, Artico H, et al. Ultrasonography of the brachial plexus, normal appearance and practical applications. Diagn Interv Imaging. 2014;95:259–75.
16. Canella C, Demondion X, Abreu E, et al. Anatomical study of spinal accessory nerve using ultrasonography. Eur J Radiol. 2013;82(1):56–61.
17. Kennedy E, Albert M, Nicholson H. The fascicular anatomy and peak force capabilities of the sternocleidomastoid muscle. Surg Radiol Anat. 2017;39(6):629–45.
18. Kelley MJ, Kane TE, Leggin BG. Spinal accessory nerve palsy: associated signs and symptoms. J Orthop Sports Phys Ther. 2008;38:78–86.
19. Kakkar C, Shetty CM, Koteshwara P, Baijpai S. Telltale signs of peripheral neurogenic tumors on magnetic resonance imaging. Indian J Radiol Imaging. 2015;25(4):453–8.
20. Linda DD, Harish S, Stewart BG, Finlay K, Parusa N, Rebello RP. Multimodality imaging of the peripheral neuropathies of the upper limb and brachial plexus. Radiographics. 2010;30(5):1373–400.
21. Stephens L, Kinderknecht JJ, Wen DY. Musculocutaneous nerve injury in a high school pitcher. Clin J Sport Med. 2014;24(6):e68–9.

22. Chiavaras MM, Jacobson JA, Billone L, Lawton JM, Lawton J. Sonography of the lateral antebrachial cutaneous nerve with magnetic resonance imaging with anatomic correlation. J Ultrasound Med. 2014;33(8):1475–83.
23. Miller TT, Reinus WR. Nerve entrapment syndromes of the elbow, forearm, and wrist. AJR Am J Roentgenol. 2010;195:585–94.
24. Lee MJ, LaStayo PC. Pronator syndrome and other nerve compressions that mimic carpal tunnel syndrome. J Orthop Sports Phys Ther. 2004;34(10):601–9.
25. Strakowski JA. Ultrasound-guided peripheral nerve procedures. Phys Med Rehabil Clin N Am. 2016 Aug;27(3):687–715.
26. Sehmbi H, Madjdpour C, Shah UJ, Chin KJ. Ultrasound-guided distal peripheral nerve block of the upper limb: a technical review. J Anaesthesiol Clin Pharmacol. 2015;31(3):296–307.
27. Hide IG, Grainger AJ, Naisby GP, Campbell RS. Sonographic findings in anterior interosseous nerve syndrome. J Clin Ultrasound. 1999;27:459–64.
28. Cheung JW, Shyu JF, Teng CC, Chen TH, Su CH, et al. The anatomical variations of the palmar cutaneous branch of the median nerve in Chinese adults. J Chin Med Assoc. 2004;67(1):27–31.
29. Nagle DJ, Santiago KJ. Anomalous palmar cutaneous branch of the median nerve in the distal forearm: a case report. Hand Surg Am. 2008;33(8):1329–30.
30. Tagliafico A, Pugliese F, Bianchi S, Bodner G, Padua L, Rubino M, et al. High-resolution sonography of the palmar cutaneous branch of the median nerve. AJR Am J Roentgenol. 2008;191(1):107–14.
31. Riegler G, Pivec C, Platzgummer H, Lieba-Samal D, Brugger P, Jengojan S, et al. High-resolution ultrasound visualization of the recurrent motor branch of the median nerve: normal and first pathological findings. Eur J Radiol. 2017;27(7):2941–9.
32. Shams OE, Al-Ghanmdi SM. Isolated neuropathy of recurrent motor branch of median nerve. Neurosciences (Riyadh). 2006;11:326–8.
33. Duggal A, Anastakis DJ, Salonen D, Becker E. Compression of the deep palmar branch of the ulnar nerve by a ganglion. Hand. 2006;1:98–101.
34. Kim SS, Kim JH, Kand HI, Lee SJ. Ulnar nerve compression at Guyon's canal by an arteriovenous malformation. J Korean Neurosurg Soc. 2009;45:57–9.
35. Le Corroller T, Bauones S, Acid S, Champsaur P. Anatomical study of the dorsal cutaneous branch of the ulnar nerve using ultrasound. Eur J Radiol. 2013;23:2246–51.
36. Wajid H, LeBlanc J, Shapiro DB, Delzell PB. Bowler's thumb: ultrasound diagnosis of a neuroma of the ulnar digital nerve of the thumb. Skelet Radiol. 2016;45:1589–92.
37. Meng S, Tinhofer I, Weninger WJ, Grisold W. Anatomical and ultrasound correlation of the superficial branch of the radial nerve. Muscle Nerve. 2014;50(6):939–42.
38. Andreisek G, Crook DW, Burg D, Marincek B, Weishaupt D. Peripheral neuropathies of the median, radial, and ulnar nerves: MR imaging features. Radiographics. 2006;26(5):1267–87.
39. Choi S-J, Ahn JH, Ryu DS, Kang CH, Jung SM, Park MS. Ultrasonography for nerve compression syndromes of the upper extremity. Ultrasonography. 2015;34(4):275–91.
40. Chien AJ, Jamadar DA, Jacobson JA, Hayes CW, Louis D. Sonography and MR imaging of posterior interosseous nerve syndrome with surgical correlation. AJR Am J Roentgenol. 2003;181:219–21.